The eggshell membrane as a barrier membrane for guided bone regeneration

Faisal F. Alotaibi, Zainab M. AlFaltawi, Sharon R. Oyhanart, Jonathan C. Knowles, Francesco D'Aiuto & David Y. S. Chau

View supplementary material ↗

Published online: 09 Aug 2025.

Submit your article to this journal ↗

View related articles ↗

View Crossmark data ↗

RESEARCH ARTICLE

The eggshell membrane as a barrier membrane for guided bone regeneration

Faisal F. Alotaibi[a,b,c], Zainab M. AlFaltawi[a,c,d], Sharon R. Oyhanart [ID][a], Jonathan C. Knowles [ID][a], Francesco D'Aiuto[c] and David Y. S. Chau [ID][a]

[a]Division of Biomaterials and Tissue Engineering, UCL Eastman Dental Institute, London, UK; [b]Department of Oral and Maxillofacial Surgery and Diagnostic Sciences, College of Dentistry, Prince Sattam bin Abdulaziz University, Alkharj, Saudi Arabia; [c]Periodontology Unit, UCL Eastman Dental Institute, London, UK; [d]Periodontal Department, College of Dentistry, University of Babylon, Babylon, Iraq

ABSTRACT

Background: The eggshell membrane (ESM) is a natural resource with a distinct design and composition, offering structural features consistent with barrier membranes used in guided bone regeneration (GBR), making it a promising candidate for this application. This study aims to assess the feasibility of chicken and duck ESMs as GBR alternatives by comparing them with resorbable porcine-derived collagen (Porcine CM, Bio-Gide®) and non-resorbable dense polytetra-fluoroethylene (d-PTFE, Cytoplast™).

Methods: ESMs were extracted using a standardized protocol. Membranes were then analyzed using scanning electron microscopy (SEM), Fourier-transform infrared spectroscopy (FTIR), differential scanning calorimetry (DSC), dynamic mechanical analysis (DMA), contact angle measurements (CAM), and cell culture-based assays.

Results: FTIR revealed similar collagen spectra among membranes. SEM showed structural similarities between ESMs and Bio-Gide. DSC indicated integrity maintenance at 37°C and varied storage conditions. CAM testing demonstrated collagen-based membranes' higher hydrophilicity compared to d-PTFE. DMA analysis showed duck ESM's superior tensile strength and Young's modulus compared to chicken ESM and porcine CM. Biological evaluation revealed high compatibility with human gingival fibroblasts for all materials.

Conclusion: Findings illustrate a novel sustainable biomaterial that could be utilized for GBR and other periodontal therapies, particularly in its capacity to function as a physical barrier consistent with the traditional role of GBR membranes.

PLAIN LANGUAGE SUMMARY

This study investigates the potential of eggshell membrane (ESM) – the thin, collagen-rich layer found between the eggshell and the egg white – as a natural barrier membrane for guided bone regeneration (GBR) in dental surgery. GBR is a widely used technique to rebuild bone in areas where it has been lost, often before placing dental implants. Barrier membranes are used to protect the healing area and prevent soft tissue from growing into the bone defect. Currently used membranes are typically made from mammalian-derived collagen or synthetic materials, which can be costly, non-sustainable, or raise ethical concerns.

In this research, ESM from chicken and duck eggs was isolated and compared with two commercially available membranes: a resorbable porcine collagen membrane and a non-resorbable synthetic membrane. The membranes were analyzed for their physical properties, such as thickness, strength, surface structure, and wettability, as well as their compatibility with human gum cells in laboratory tests. The findings showed that ESM has favorable structural features and supports healthy cell growth, indicating its promise as a barrier material.

Although further testing, including studies in animals and bone-related cells, is needed, ESM could offer a sustainable, low-cost alternative for GBR, helping advance dental regeneration practices in a more accessible and eco-conscious direction.

The Eggshell Membrane as a Barrier Membrane for Guided Bone Regeneration

1. Introduction

Guided bone regeneration (GBR) is a fundamental technique within the field of implant dentistry, required in about 40% of all dental implant cases [1,2], particularly when bone volume is compromised due to trauma, pathology, or tooth loss. The technique relies on barrier membranes to prevent soft tissue ingrowth and to establish a secluded environment supportive to selective bone regeneration [3]. The characteristics of an ideal membrane for GBR extend beyond the barrier effect to include biocompatibility, biological activity, proper porosity, mechanical strength, exposure tolerance, and biodegradability. Membranes should also be rigid enough to resist compression by overlying tissues, possess handling properties like elasticity, and be easily shaped to fit the desired bone contour [4].

Collagen-based membranes have been extensively utilized in GBR procedures due to their excellent biocompatibility, bioresorbability, natural source, and ability to support new bone formation. These membranes are derived mainly from animal or human sources and provide a scaffold that promotes cell attachment, proliferation, and differentiation-key processes for bone healing. In addition, collagen membranes possess distinct physical characteristics, such as tensile strength, flexibility, and a porous structure that facilitates nutrient exchange and vascularization, further supporting the regeneration process. Despite their widespread use, collagen membranes have limitations, such as variable resorption rates, potential antigenicity, and high cost [5]. Dense polytetrafluoroethylene (d-PTFE) membranes represent another category of materials employed in GBR. Unlike collagen membranes, d-PTFE membranes are non-resorbable and require removal in a subsequent surgical procedure. Their primary advantage lies in their ability to maintain space effectively while being impervious to cellular and bacterial infiltration. However, the need for a second surgery for membrane removal, thereby increasing both cost and patients' discomfort, along with the increased susceptibility to exposure and infection, are significant drawbacks [6–8].

Avian eggshell membrane (ESM) is a thin, bilayered, highly collagenous, fibrous membrane that lies in between the mineralized eggshell and egg white (albumin) [9,10]. It acts as a natural scaffold for biomineralization during the formation of an eggshell, with a distinctive fibrous texture on both its outer and inner surfaces. This structural design facilitates the mineralization of eggshells on the outer side while preventing the mineralization of egg yolk on the inner side [11]. ESMs, mainly from chicken, have been explored for their utility across various medical fields, including dermatology [12], ophthalmology [13], cardiology [14], and regenerative medicine of nerves [15], bones [16], and cartilages [17]. These studies have highlighted several mechanical and biological characteristics of ESMs, such as excellent biocompatibility, unique physical properties, and a rich composition of bioactive molecules, which could make them suitable for GBR, offering a sustainable, cost-effective, and readily available resource of membranes.

Previous studies have investigated engineered GBR membranes incorporating ESM with synthetic polymers and bioceramics [18,19]. While these show promise as affordable, eco-friendly alternatives to collagen membranes, the authors emphasize the need for thorough physicochemical and biological characterization to confirm clinical viability. Earlier studies also evaluated chemically treated ESMs in animal GBR models, though results were inconsistent [20,21]. Hence, this study aims to assess whether ESMs from chickens and/or ducks can provide a viable and sustainable alternative in GBR by comparing their mechanical and biological characteristics with membranes in current clinical practice.

2. Materials and methods

2.1. Materials

Free range, large, brown chicken eggs (Heritage Breeds™, Copper Marans) and free range, king sized, white duck eggs (Gladys-May's Braddock Whites, Clearance Court) were purchased from local supermarket (Waitrose & Partners, London, UK). Commercially available, porcine-derived resorbable collagen

Article highlights

- This is the first study to evaluate the structural, mechanical, and biological characteristics of native chicken and duck eggshell membranes (ESMs) as potential barrier membranes for guided bone regeneration (GBR).
- ESM is a naturally bilayered, collagen-rich membrane derived from food industry waste, offering a sustainable, cost-effective, and xeno-free alternative to mammalian-derived or synthetic GBR membranes.
- Structural characterization by scanning electron microscopy revealed a distinct Janus architecture in ESM, with a dense outer surface and porous inner surface—resembling clinically established bilayer GBR membranes.
- Thermal and mechanical analysis confirmed the stability of ESM under various physiological and storage conditions.
- In vitro cell proliferation assays using human gingival fibroblasts (hGF) demonstrated that both chicken and duck ESMs are non-cytotoxic and support healthy cell growth, comparable to Bio-Gide® and d-PTFE membranes.
- ESM thickness is significantly lower than that of currently widely used clinical membranes, yet its handling properties and surface structure suggest suitability for use in soft-tissue exclusion.
- The study establishes a foundation for further development of ESM-based GBR materials. Future work should include animal studies, evaluation of osteogenic potential on the rough membrane surface, and exploration of regulatory pathways to support the clinical translation of ESM as a novel resorbable barrier membrane.

membrane (Bio-Gide®, Geistlich Biomaterials, Baden-Baden, Germany) and synthetic non-resorbable d-PTFE membrane (Cytoplast™ TXT-200; Osteogenics Biomedical, Lubbock, Texas, USA) were obtained. Acetic acid, ≥99% was purchased from Fisher Scientific (Loughborough, Leicester, UK). Penicillin/streptomycin (P/S) was obtained from Sigma-Aldrich (Poole, UK). Human gingival fibroblasts (HGF-1) cell line was utilized (CRL-2014, ATCC, LGC Standards, Middlesex, UK). Dulbecco's modified Eagle medium (DMEM), fetal bovine serum (FBS), and phosphate-buffered saline (PBS, pH 7.2) were purchased from Sigma-Aldrich (Merck, Dorset, UK). CellTiter 96®AQueous One Solution Cell Proliferation assay (G3582) and the CytoTox 96® Non-radioactive Cytotoxicity Assay (G1780) were purchased from Promega (Southampton, UK).

2.2. ESM extraction

The extraction process is shown in Figure 1. An optimized isolation protocol, as previously reported [13], was followed to extract the chicken and duck ESM membranes. In brief, eggs were meticulously washed with distilled water then submerged in 0.5 M acetic acid solution at room temperature (~19°C). After 44 h, eggs were removed, washed with distilled water, and cleaned of any remaining residual shell (calcium carbonate) manually. The albumin and yolk were then removed, and the extracted membranes were washed, fully immersed in PBS, to prevent dehydration, and refrigerated at 4°C before use.

2.3. Membrane characterization

2.3.1. Thickness

Membrane thickness was measured using a digital caliper (Fowler/Sylvac Ultra-Cal III; Fred V. Fowler, Newton, Massachusetts, US). Three samples of each membrane type were assessed; for each sample, thickness was measured at three random locations and recorded at the first contact, avoiding excessive pressure of the caliper jaws. Values were rounded to the nearest 0.01 mm and reported as mean and SD for each membrane.

2.3.2. FT-IR

The inner and outer surfaces of the membranes were chemically characterized by examining the vibrational modes of their functional groups via Fourier Transform Infrared Spectroscopy (FT-IR) using an attenuated total reflectance (ATR) diamond crystal (MK1 Golden Gate, Specac Inc., Orpington, UK) coupled to a Perkin Elmer Spectrum One FT-IR spectrometer. Spectra were obtained at room temperature (19°C) between 400 and 4000 cm^{-1} at a resolution of 8 cm^{-1} and as the result of four scans per sample and processed using the software Spectrum IR v10.7.2.1630 (Perkin Elmer). A background spectrum was collected immediately before placing the ESM onto the diamond crystal to measure the signal contribution of the instrument and environment to the membranes' spectra.

2.3.3. SEM

The surface morphological characteristics of the specimens were analyzed using a scanning electron microscope (SEM) (Zeiss EVO HD, Jena, Germany). Prior to imaging, samples were cut into 12 mm discs, mounted on aluminum stubs using adhesive carbon tabs (Agar Scientific, Stansted, UK), and coated with 95% gold and 5% palladium using a Polaron E5000 Sputter Coater (Quorum Technologies, Laughton, UK). Inner and outer surfaces of the membranes were imaged at magnifications of 500x and 2000x and accelerating voltage of 5 kV and working distance (WD) of 10.15 mm ±0.23.

2.3.4. Thermal analysis

Three weighted (~10 mg) samples of each membrane were placed in into hermetic Tzero® Pans and Lids (TA Instruments, New Castle, Delaware, USA) and submitted to a temperature ramp of 0–400°C, at a rate of 20°C/min under a continuous flowrate of nitrogen gas using a differential scanning calorimeter (DCS25, TA Instruments, New Castle, Delaware, USA). An empty pan was used as reference during each scan and track variations in heat capacity of each membrane were analyzed using TRIOS software (TA Instruments).

2.3.5. Wettability

Hydrophilicity of both inner and outer surfaces of each membrane were determined by contact angle measurements using the sessile drop method/optical contact angle profiling. A droplet of distilled water (~2 µL) was deposited on the flat membrane surface, and the contact angle was measured using CAM 200 optical angle meter (KSV Instruments Ltd., Helsinki, Finland) at room temperature (~19°C). Each value of the contact angle was calculated as an average of three different readings taken under the same conditions.

2.3.6. Mechanical analysis

Three rectangular samples of each membrane (7 mm by 15 mm, soaked in PBS for 2 min) were subjected to tensile strength testing at room temp (~19°C). The ultimate tensile
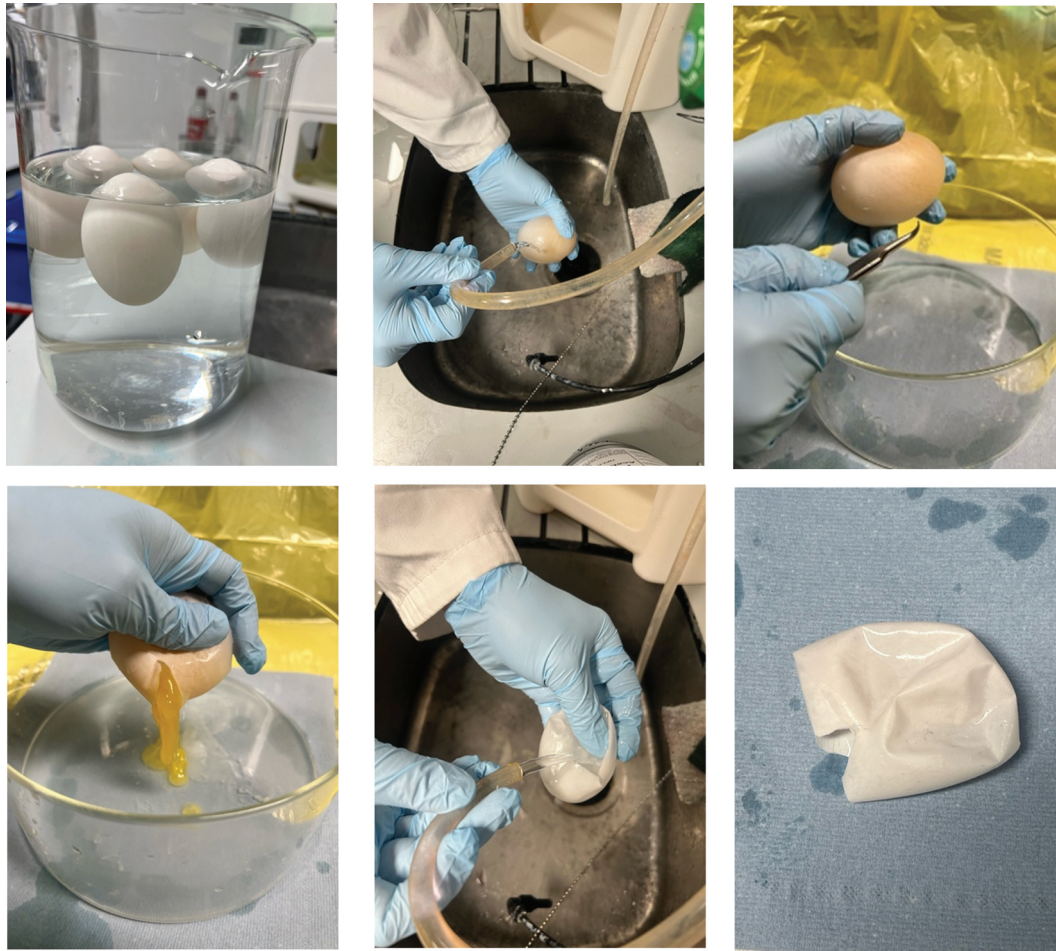
Figure 1. Extraction protocol of the ESM (top: L-R): (1) Eggs submerged in 0.5 M acetic acid solution for 44 h. (2) Washed with distilled water. (3) Pierced with tweezers. (bottom L-R, 4) Yolk and albumen disposed safely. (5) Extracted ESM rinsed with water. (6) Fully extracted ESM samples (method adapted from Mensah et al., [13]).

strength and % elongation at break were obtained using the Dynamic Mechanical Analysis (DMA850, TA Instruments, New Castle, Delaware, USA) setup and TRIOS software. Young's Modulus was extrapolated from the linear slope of the stress-strain curves. The tensile strength (UTS) and elongation at break were calculated as stated below in Equation 1:

$$UTS(MPa) = \frac{Maximum\ load\ at\ break(N)}{Cross-sectional\ area(m2)}$$

$$Elongation(\%) = \frac{Break\ length - Initial\ length}{Initial\ length} x100 \quad (1)$$

2.4. Biological characterization

Human gingival fibroblasts (hGF) were cultured with DMEM (high glucose 4500 mg/L, L-glutamine, sodium pyruvate, and sodium bicarbonate, liquid, sterile-filtered, suitable for cell culture) supplemented with 10% (v/v) FBS and 1% penicillin-streptomycin under standard humidified cell culture conditions 37°C in 5% CO_2. A standard trypsinization protocol (i.e., 1% (v/v) Trypsin-EDTA) every 3 days was followed upon cells reaching sub-confluence (80–90%). Cells at passage 8 (P8) were used in subsequent experiments. Sample preparation included cutting the membranes into 5 mm discs using a biopsy punch before placing them into 96-well plates

(Corning Costar™, Thermo Fisher, Paisley, UK) and sterilizing them under UV light (Steristorm 2537a, Daro UV systems, Dartford, UK) for 20 min, each side. Samples were then soaked in PBS for 5 min and the hGF were seeded on the smooth sides of the membranes (chicken ESM, duck ESM, porcine derived CM, d-PTFE) or directly on tissue culture plastic as a control, at a density of 2×10^4 cells/cm2 in 300 μL of the complete growth media and incubated in 37°C and 5% CO_2. Each group consisted of six replicates.

2.4.1. Cell Proliferation (MTS) Assay

CellTiter 96®AQueous One Solution Cell Proliferation assay (Promega, Southampton, UK) was used to evaluate the metabolic activity of the cells according to the manufacturer protocol. Briefly, following incubation periods of 1, 3, 7, and 14 days, 75 μL of Triton-X lysis buffer was added to one control sample to produce a negative control and incubated at 37°C and 5% CO_2 for 40 min. Then, 50 μL of the culture media was transferred to a new 96-well plate to be used for LDH assay as described below. Thereafter, 50 μL of CellTiter One reagent was added to the remaining 250 μL of the culture media in each well. The plate was then wrapped in aluminum foil and incubated at 37°C and 5% CO_2 for 2 h. Next, 100 μL of media

from each well was transferred to a new 96-well plate and read at 490 nm on the Infinite M200 (Tecan, Zürich, Switzerland) plate reader. Relative metabolic activity (cell viability) was normalized to the control and calculated using the formula below (see Equation 2) with (−) referring to the negative control, i.e., untreated cells.

$$Cell\ viability(\%) = \frac{Sample\ absorbance - blank\ absorbance}{Control(-)absorbance - blank\ absorbance} x100 \quad (2)$$

2.4.2. Cytotoxicity (LDH) assay

CytoTox 96® Non-radioactive Cytotoxicity Assay (Promega. Southampton, UK) was used to evaluate the Lactate dehydrogenase (LDH) release from the cells according to the manufacturer protocol. In summary, 50 μL of Triton-X lysis buffer was added to one control sample to produce a negative control and incubated at 37°C and 5% CO_2 for 40 min before transferring 50 μL of the culture media to a new 96-well plate, as described above. A similar quantity (50 μL) of CytoTox 96® Non-radioactive Cytotoxicity Assay reagent was added to each well. The plate was then covered with aluminum foil, to protect from light, and incubated at room temperature (~19°C) for a period of 30 min; once elapsed, absorbance was read at 490 nm on the Infinite M200 (Tecan) plate reader. Relative LDH release (cytotoxicity) was calculated as a percentage relative to the positive control (+), cells treated with Triton-X-100 (0.015 w/v) only, using the formula as shown in Equation 3.

$$Cytotoxcity(\%) = \frac{Sample\ absorbance - control\ absorbance}{Control(+)absorbance - blank\ absorbance} x100 \quad (3)$$

2.4.3. Live/Dead cell viability assay

To visualize cells viability/death and to support the quantitative analysis, three 5 mm discs of each of the chicken ESM, duck ESM, porcine derived CM, d-PTFE were prepared and cultured as described above. The samples were then stained with Live/Dead™ staining (Invitrogen Life Technologies, ThermoFisher, Leicester, UK) were used according to the manufacture protocol. In brief, at the relevant time point, the media containing the seeded samples was discarded, and the samples were rinsed

with PBS. The stain was prepared by adding 20 μL of EthD-1 (2 mM) stock solution to 10 mL PBS, combined with 5 mL Calcein AM (4 mM) stock solution. After 1, 3, 7 and 14-days incubation, 100 μL of the stain was added to each sample and incubated at (~19°C) for 20 min in a 96-well plate covered with aluminum foil. The viability/death of the cells was visualized using fluorescence microscopy (LEICA Instruments, Milton Keynes, UK) on Image Capture Pro software.

2.5. Statistical analysis

Quantitative results are expressed as mean and standard deviation (SD). Experiments were performed in triplicate, and generated data were analyzed using GraphPad Prism version 10. A one-way or two-way analysis of variance (ANOVA) with Bonferroni's Multiple Comparison posttest was carried out to compare sample means and variance among treatment groups and to negative controls. Results with $p < 0.05$ (*), $p < 0.01$ (**), $p < 0.001$ (***) were considered statistically significant.

3. Results

3.1. Membrane characterization

3.1.1. Thickness
Table 1 and Figure 2(A) presents the thickness measurements of four types of membranes. The data revealed statistically significant differences in thickness across all membrane types, with the porcine-derived CM being the thickest at 0.45 mm (±0.005), followed by the d-PTFE membrane at 0.24 mm (±0.003), the duck Eggshell Membrane (ESM) at 0.14 mm (±0.01), and the chicken ESM being the thinnest at 0.1 mm (±0.02).

3.1.2. Thermal properties
Table 1 and Figure 2(B) present thermal profiles of the four membranes. Collagen based membranes (i.e., chicken ESM, duck ESM and porcine derived CM) showed relatively similar profiles with an average endothermic decomposition peaks ranging from 130 to 170°C while for the d-PTFE membrane, the average value was significantly higher at 340°C ($p < 0.001$).

3.1.3. Mechanical properties
Table 1 and Figures 2(C–F) F, respectively, summarize UTS, strain (%), elongation (%), and Young's Modulus measurements of the chicken ESM, duck ESM, and porcine-derived membranes. Data on the d-PTFE membrane could not be

Table 1. Comparative analysis of membrane thickness, thermal profile, and mechanical properties of membrane samples ($n = 3$).

		Chicken ESM	Duck ESM	Porcine CM	d-PTFE
Membrane Thickness (mm)	Minimum	0.082	0.126	0.442	0.238
	Maximum	0.120	0.145	0.451	0.245
	Mean	0.099 ± 0.019	0.136 ± 0.01	0.446 ± 0.005	0.242 ± 0.003
Thermal Profile	Onset Temp (°C)	162.5 ± 9.3	159.3 ± 6.4	112.1 ± 16.9	340.7 ± 12.5
	Peak Temp (°C)	169.5 ± 5.2	160.1 ± 9.7	131.6 ± 17.9	347.2 ± 8.6
	Enthalpy (J/g)	1753.2 ± 167.1	1601.6 ± 103.8	7614 ± 159.3	202.3 ± 41.7
Mechanical properties	UTS (MPa)	2.955 ± 0.979	4.870 ± 1.557	0.987 ± 0.335	NA
	Strain (%)	47.79 ± 9.69	63.01 ± 2.25	59.69 ± 12.39	NA
	Elongation (%)	38.650 ± 9.261	53.320 ± 1.910	49.330 ± 13.460	NA
	Young's Modulus (MPa)	4.028 ± 1.182	8.796 ± 3.759	1.967 ± 0.807	NA

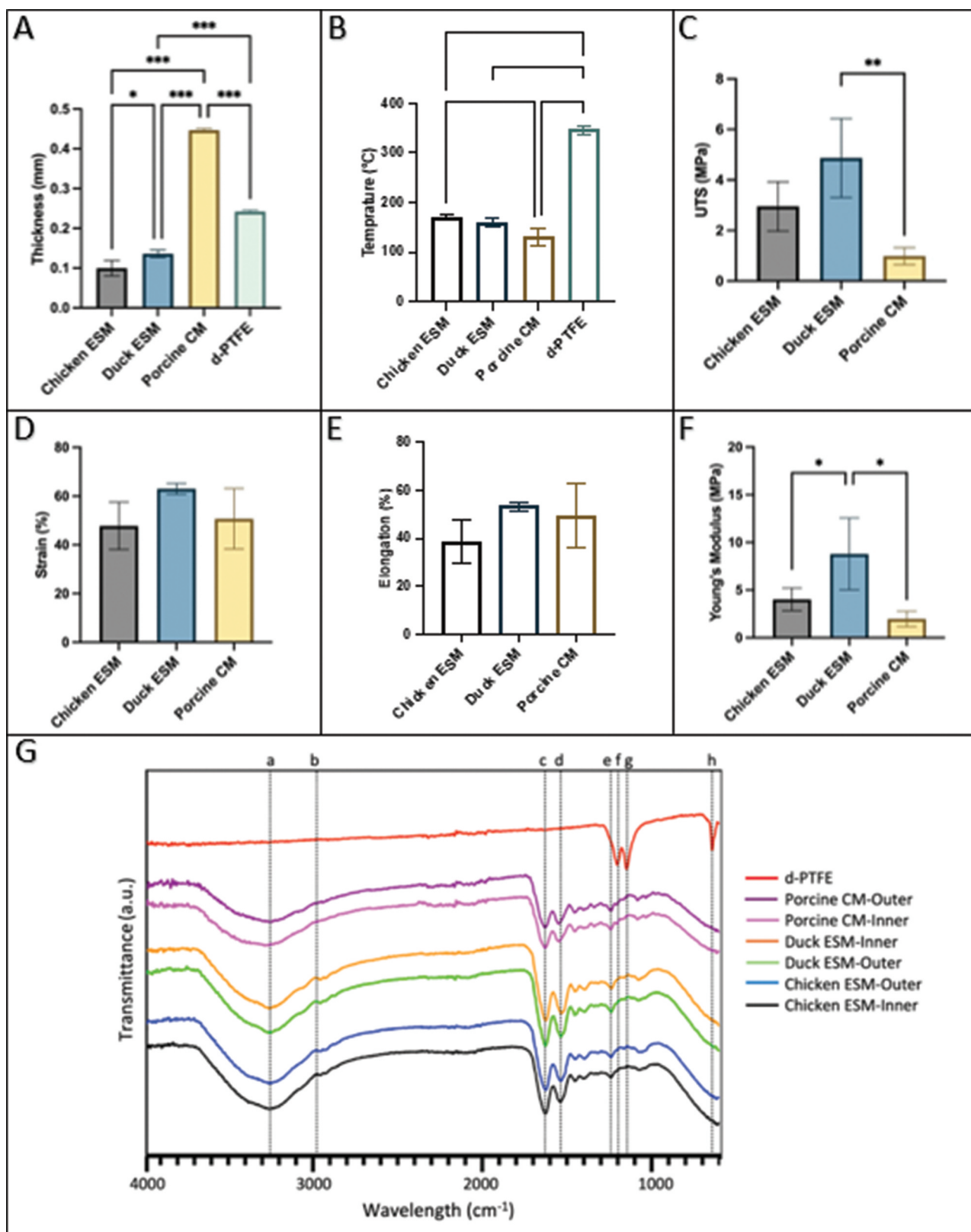Abbreviations: UTS: Ultimate tensile strength.

Figure 2. Physical and chemical characterization. (A) measurements of membranes' thicknesses measured using a digital caliper. (B) endothermic decomposition peaks obtained via differential scanning calorimetry (DSC) operating with temperature ramp of 0–400°C, at a rate of 20°C/min under a continuous flowrate of nitrogen gas. (C) ultimate tensile strength (UTS), (D) strain, (E) elongation, and (F) Young's modulus obtained via dynamic mechanical analysis (DMA) of rectangular (7 x 15 mm) samples at room temp (~19°C). (G) Fourier transform infrared spectrophotometer (FT-IR) spectra obtained at room temperature (19°C) between 400 and 4000 cm^{-1} at a resolution of 8 cm^{-1}. Vertical lines identify distinctive peaks associated with the bands; (a) amide a band observable at 3280 cm^{-1}, (b) amide B band observable at 2990 cm^{-1}, (c) amide I observable at 1620 cm^{-1}, (d) amide II observable at 1530 cm^{-1}, (e) amide III observable at 1240 cm^{-1}, (f) CF2 asymmetric stretching observable at 1195 cm^{-1}, (g) CF2 symmetric stretching observable at 1130 cm^{-1}, and (h) CF2 wagging observable at 630 cm^{-1}. (A-F) data are shown as mean ± SD from triplicate experiments. Statistical analysis used one-way ANOVA with Bonferroni's post-tests. Significance levels are $p < 0.05$ (*), $p < 0.01$ (**), $p < 0.001$ (***). Abbreviations: CM: collagen membrane; d-PTFE: dense-polytetrafluorethylene; ESM: eggshell membrane; UTS: ultimate tensile strength.

obtained as the DMA machine reached its 28 mm motion limit (i.e., 300% elongation of the 7 mm long d-PTFE membrane sample) before reaching the membrane break point. Nevertheless, this demonstrates the d-PTFE membrane's substantial superiority in terms of mechanical properties when compared to the chicken ESM, duck ESM, and porcine-derived CM. Among the natural collagen-derived membranes, significant differences were observed only with regard to the UTS, with the duck ESM outperforming the porcine CM, and Young's Modulus, where this ESM exhibited higher values than both the chicken ESM and the porcine CM. When making comparisons among the latter, duck ESM had higher UTS than the porcine derived CM ($p < 0.01$) and higher Young'smodulus than the chicken ESM and porcine derived CM ($p < 0.05$). All other comparisons were not statistically significant.

3.1.4. Biochemical properties

Figure 2(G) presents the FT-IR spectra of the inner and outer surfaces of four membrane types. For collagen-based membranes (chicken ESM, duck ESM, and porcine CM), Amide A (3280 cm^{-1}) and Amide B (2990 cm^{-1}) bands indicate hydrogen bonds and C-H stretching. Amide I, II, and III bands (1620 cm^{-1}, 1530 cm^{-1}, and 1240 cm^{-1}) reflect high collagen content. The e-PTFE membrane shows strong bands at 1195, 1130, and 630 cm^{-1}, characteristic of CF2 asymmetric stretching, CF2 symmetric stretching, and CF2 wagging.

3.1.5. Wettability

Contact angle measurements of inner and outer surfaces of the four membranes. An expected more hydrophilic behavior was noted in the natural collagen-based membranes (i.e., chicken ESM, duck ESM, and porcine derived CM) compared to the synthetic d-PTFE membrane, as reflected by the latter displaying values >90° (Appendix Figure 1).

3.1.6. Morphology

Figure 3(A) displays the SEM images of both surfaces of each membrane. For the chicken ESM, duck ESM, and porcine-derived CM, distinct structural differences are evident between the two surfaces of each membrane, with one side presenting a smooth architecture and the other, a rough texture. The smooth surfaces feature a flat, non-porous morphology with multiple circular bulges visible at higher magnification. Conversely, the rough surfaces reveal a dense, haphazard fibrillar network with microporous structures.

Further analysis showed that chicken and duck ESMs had thinner fibers and more micropores compared to porcine CM (Figures 3(B,C)). Statistical analysis revealed significant differences in pore and fiber sizes and quantities. The d-PTFE membrane was non-porous with one textured side featuring hexagonal dimples (~150 μm).

3.2. Biological characterization

3.2.1. Cell Proliferation (MTS) Assay

Figure 4(A) depicts the relative metabolic activity of the human fibroblast cells expressed as a percentage of cell untreated and assessed using the MTS assay following in vitro culture on the four types of membranes for up to 14 days. The metabolic activity of fibroblasts cultured on ESMs consistently trended close to or even slightly higher that of the untreated control group throughout the 14-day period. While these differences did not reach statistical significance ($p > 0.05$), the upward trend – most notably at Day 14—suggests a favorable cellular response to the ESM materials.

3.2.2. Cytotoxicity (LDH) Assay

Figure 4(B) shows the relative LDH release from the seeded cells expressed as a percentage of cells treated with Triton-X and assessed using the LDH assay on the four membranes up to 14 days. Statistically significant differences were noted at the 3-day mark between the chicken ESM and the porcine CM, and at 7 days between the chicken and duck ESMs. By 14 days, however, the differences in LDH release among the treatment groups leveled off, showing no statistical difference. At this time point, all groups exhibited a decrease in LDH release in comparison to earlier observations.

3.2.3. Live/dead cell viability assay

Cells seeded on the four types of membranes were stained with a Live/Dead^{TM} cytotoxicity assay kit to visualize the in vitro viability and cytotoxicity (Figure 4(C)). After 14 days of incubation with each of the membranes exhibited very high cell viability and contained minimal dead cells.

4. Discussion

This study aims to compare selected mechanical and biological characteristics of chicken and duck eggshell membranes with two widely used membranes in GBR. To our knowledge, this is the first study to directly compare ESMs with membranes commonly used in GBR: (i) resorbable porcine-derived CM (Bio-Gide) and (ii) non-resorbable d-PTFE membrane (Cytoplast). Resorbable membranes are typically used for cases of horizontal bone defects with no or minimal vertical components, while non-resorbable membranes are used for more extensive cases requiring longer barrier function, such as advanced vertical bone defects.

Measurements of membrane thicknesses shows that chicken ESM (0.10 mm ± 0.02) and duck ESM (0.14 mm ± 0.01) are approximately one-fourth the thickness of Bio-Gide and half that of Cytoplast. A study by Bubalo, Lazić [22] assessing the effect of thickness of collagen-based resorbable membranes on bone regeneration, demonstrated that the use of membranes with thicknesses of 0.1 mm and 0.2 mm was successful in enhancing bone defect repair in study dogs, showing significantly more newly formed bone compared to negative controls. Additionally, the relatively thin profile of chicken and duck ESMs compared to the controls affords opportunities for enhancing their mechanical properties, such as through techniques like membrane stacking or integration with other materials, without concern for excessive thickness. Nevertheless, such approaches must be carefully considered due to the Janus architecture of ESM, where surface orientation is functionally significant. Improper stacking may compromise this directional functionality. The lack of direct ESM-based GBR products and
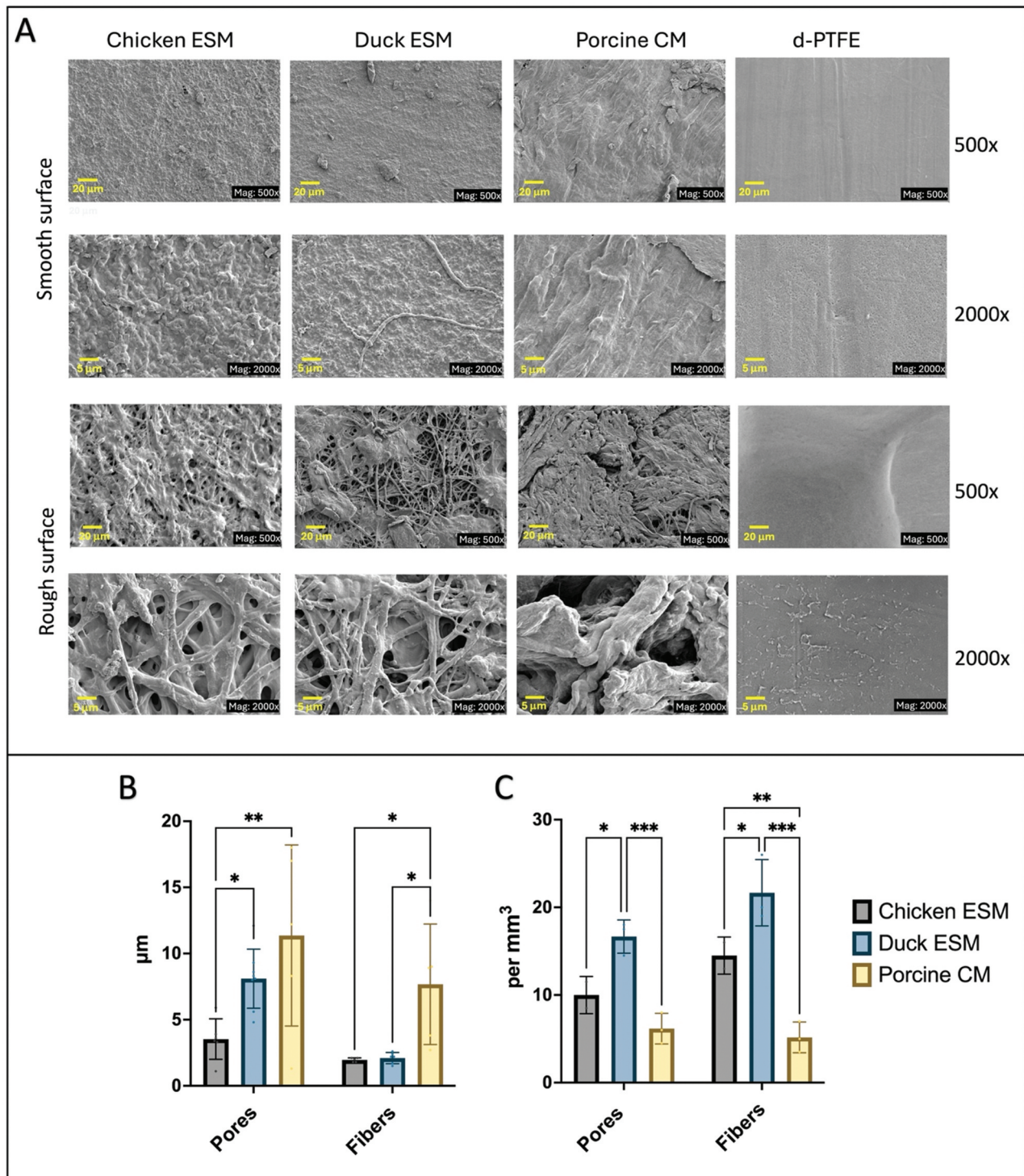
Figure 3. Morphological characterization. (A) scanning electronic microscopic (SEM) images of the smooth and rough surfaces of samples cut into 12 mm discs, mounted on aluminum stubs, and coated with 95% gold and 5% palladium at magnification of 500× and 5000×, accelerating voltage of 5 kV and working distance of 10.15 mm ±0.23. (B) Diameter; and (C) quantity of pores and fibers found within the samples. (B, C) data are shown as mean ± SD from triplicate experiments. Statistical analysis used two-way ANOVA with Bonferroni's posttests. Significance levels are $p < 0.05$ (*), $p < 0.01$ (**), $p < 0.001$ (***). Abbreviations: CM: collagen membrane; d-PTFE: dense-polytetrafluoroethylene; EHT: electron high tension; ESM: eggshell membrane; Mag: magnification; WD: working distance.

limited in vivo data to date may, in part, reflect these challenges. Therefore, in vivo studies are essential to assess whether ESMs, either in their unmodified state or in engineered formats, can meet the mechanical and regenerative demands of GBR.

FTIR analysis was performed to inspect the chemical composition of the four types of membranes. The IR spectra taken from the inner and outer surfaces of the chicken ESM, duck ESM, and porcine derived CM (Bio-Gide) revealed the presence of amide A, amide B, amide I, amide II, and amide III bands, characteristic of the membranes' high protein content, specifically collagen [23]. The eggshell membrane comprises two layers; a type I collagen predominant outer layer, in contact with the eggshell, and a type
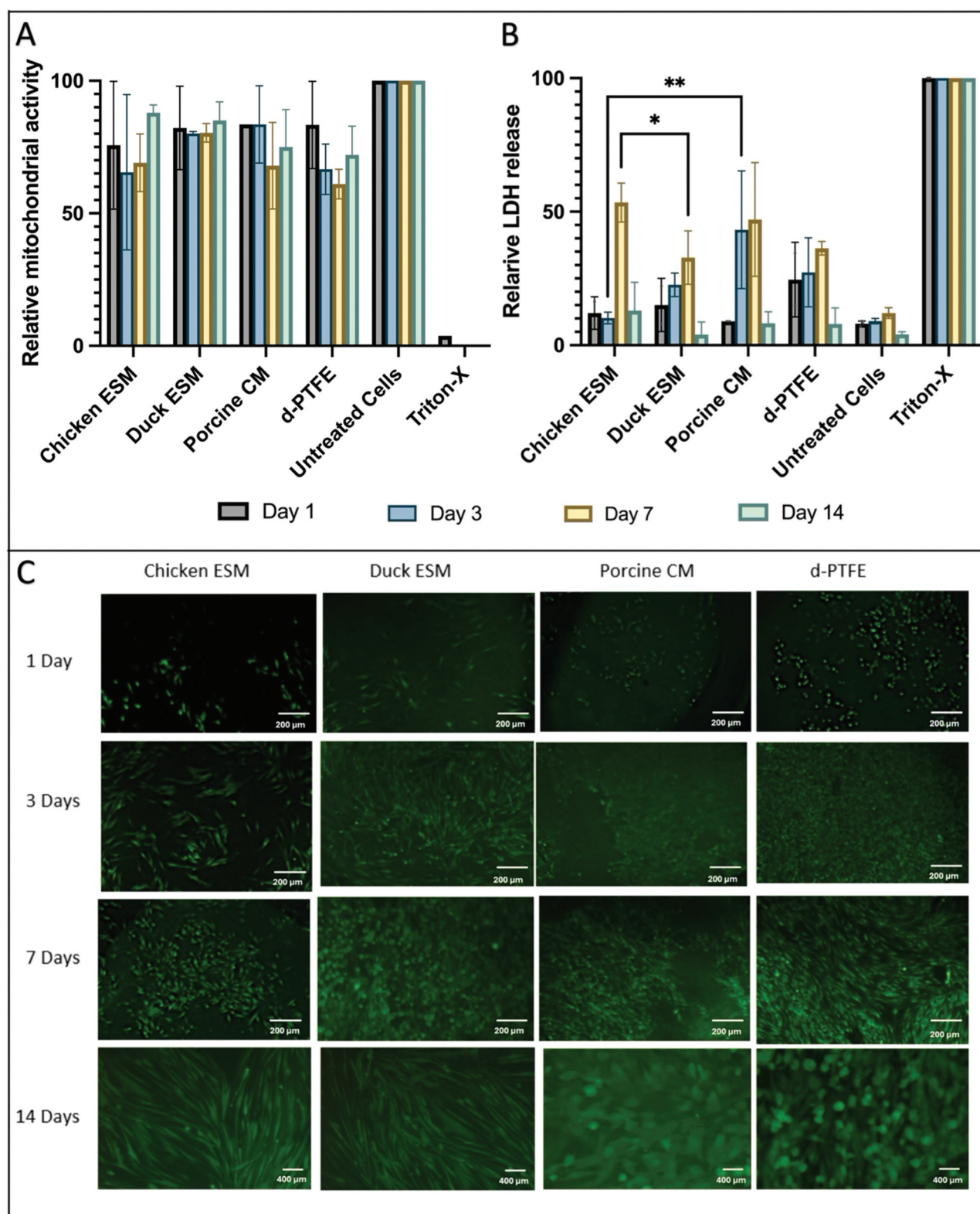
Figure 4. Biological characterization. (A) cell metabolic activity; and (B) LDH release of cells cultured on samples at 10^4 cells per well density over 14 days. (C) viability and cytotoxicity demonstrated by Live/Dead™ staining of cells seeded on samples for a 14-day duration under the fluorescence microscope with the stain identifying live cells as fluorescent green and dead cells to fluoresce red. (A, B) data are shown as mean ± SD from triplicate experiments. Statistical analysis used two-way ANOVA with Bonferroni's post-tests. Significance levels are $p < 0.05$ (*), $p < 0.01$ (**), $p < 0.001$ (***). Abbreviations: CM: collagen membrane; d-PTFE: dense-polytetrafluorethylene; ESM: eggshell membrane; LDH: lactate dehydrogenase assay.

V predominant inner layer, in contact with the albumin [24,25]. Type X collagen can also be found in both layers of the ESM [25]. Bio-Gide, on the other hand, is composed mainly of type I and III collagen [26,27]. Moreover, the presence and clarity of the amide I, II, and III bands suggest that the triple-helical structure of collagen was largely retained following extraction. Nonetheless, future studies should incorporate additional structural analyses, such as circular dichroism or the amide III/I ratio, to confirm preservation of native collagen and rule out partial gelatinization resulting from acid exposure.

Interestingly, SEM imaging showed that the structural morphology of the chicken and duck ESMs, in their unmodified state, exhibits a remarkable similarity to the intentionally engineered Bio-Gide membrane. This analysis showed that all three collagen-based membranes exhibit a bilayered structure, featuring a non-porous and compact layer on one side, contrasted with a distinctly porous layer on the other. This dual-layer architecture plays a pivotal role in collagen membranes' functionality within GBR applications. Specifically, the dense outer layer, oriented toward the soft tissue, acts as a barrier against the infiltration of epithelial cells. In contrast, the porous inner layer, facing the bone defect, facilitates tissue integration and bone regeneration [4]. Additionally, the inclusion of a dense layer in the membrane is linked to a decelerated biodegradation process, thereby extending the membrane's barrier effect [28]. The porosity of GBR membranes is also crucial for their function, with micro-porosity ranging from 5 to 20 µm being deemed optimal. This size range supports selective cellular migration and the transport of vital biomolecules while preventing larger entities' passage, which typically occurs at pore sizes of ≥30–40 µm [7,29]. However, our analysis was limited to 2D SEM-based imaging, which does not allow for direct assessment of whether these pores are open or interconnected. Future studies should apply 3D imaging or permeability testing to confirm functional pore architecture and transport dynamics.

While the SEM findings demonstrate a dense, non-porous surface layer indicative of a barrier function, no direct permeability testing (e.g., cell or bacterial occlusion assays) was conducted in this study. Therefore, the observed structural features support – but do not confirm – the functional barrier capability of ESMs. Future studies should assess the actual occlusion potential using transmigration and microbial penetration assays to fully validate ESMs as effective barrier membranes. Notably, the majority of pore sizes measured in the ESMs were within or near the optimal 5–20 µm range recommended for GBR applications, which supports their potential for selective permeability. Additionally, while recent studies have explored potential bioactive roles for GBR membranes, the foundational concept remains that of a passive barrier – preventing soft-tissue invasion and preserving space for bone regeneration [4]. Histological evidence has yet to fully define the sequential cellular and molecular events within membrane-covered defects, and the membrane's primary function continues to be physical exclusion and stabilization of the regenerative environment. Accordingly, our study focused on characterizing the ESMs' structural morphology, surface features, and compatibility with gingival fibroblasts to evaluate their potential as effective passive barriers. Future work may

explore any additional bioactive properties, but our present data align with the membrane's principal mechanical and morphological requirements [3].

DSC technique was used to assess the thermal stability of tested membrane across temperature range of 0 to 400°C. The results indicated that all tested membranes are capable of maintaining their structural integrity at body temperature, as well as under various storage conditions, including refrigeration (2–4°C), and ambient temperatures (23–25°C). Notably, the enthalpy values for chicken and duck ESMs were substantially lower than those for Bio-Gide, which may indicate a reduced degree of collagen crosslinking or partial loss of higher-order structure. This difference is potentially attributable to the acid extraction process used, which, while effective for membrane isolation, may compromise some native structural integrity. Future studies using complementary techniques such as circular dichroism or differential scanning fluorimetry could provide more direct insight into collagen stability and folding status.

CA measurements showed significantly higher hydrophilicity of the collagen-based membranes compared to the d-PTFE membrane, with the porcine CM (Bio-Gide) exhibiting the highest hydrophilicity, followed by the duck ESM then the chicken ESM. Furthermore, the findings indicated that the surfaces with higher roughness on the bilayered membranes were significantly more hydrophilic than their smoother, opposite sides, illustrating their hydrophilic nature. Indeed, according to the Wenzel model [30], roughness amplifies the inherent wettability of a surface; thus, for materials that are naturally hydrophilic, rougher surfaces will exhibit lower contact angles and enhanced hydrophilicity. This principle may also account for the superior hydrophilicity of the porcine CM over the chicken and duck ESMs, attributable to its rougher surface texture and, possibly due to its greater pore size. Typically, surfaces with low contact angles tend to promote better biocompatibility and tissue integration, whereas surfaces with high contact angles can inhibit cell adhesion and tissue repair [31,32]. This distinction has practical implications in clinical settings, recommending the smoother surface face the sutured wound area and the rougher surface toward the bone defect to enhance healing outcomes. In essence, such findings therefore favor the use of natural collagen-derived membranes compared to the d-PTFE.

The mechanical testing of the chicken ESM, duck ESM, and porcine-derived CM, alongside the d-PTFE membrane, showed significant variances in their physical properties. The inability to measure the d-PTFE membrane's tensile strength within the constraints of our DMA machine, due to its extensive elongation capacity, highlights the superior mechanical strengths inherent to the d-PTFE membrane, a quality that is well documented [7,33] and readily observable through direct manipulation. Despite its robust mechanical features, the d-PTFE membrane's non-resorbable nature, necessitating a subsequent surgical intervention for its removal when used in GBR, along with a higher susceptibility to healing complications such as exposure and infection, renders it less favorable for clinical use in comparison to resorbable collagen-based membranes [6]. The inclusion of the d-PTFE membrane as a control in our study aimed to provide a benchmark for comparison in further tests, particularly those

focusing on biological characterization. Measurements of ultimate tensile strength and Young's modulus were conducted for the collagen-based membranes, serving as crucial metrics for assessing a material's resistance to breakage and deformation, respectively. Additionally, elongation was analyzed to determine softness and elasticity, essential for membrane functionality. The membranes were tested in their wet state to mimic their application conditions in GBR practices and to account for the significant impact of hydration on the mechanical properties of collagen membranes [31]. Our findings demonstrated that the duck ESM exhibits higher tensile strength and Young's Modulus compared to the chicken ESM and porcine CM, showing its greater capacity for spatial maintenance. It is important to note that the mechanical data were obtained from three replicates per group, which provides preliminary insight but may be underpowered given the variability typically observed in biological materials. Future studies should include larger sample sizes to improve statistical reliability. Additionally, the inability to complete tensile testing on the d-PTFE membrane due to equipment limitations precluded a full mechanical comparison. Employing a universal testing machine or reporting mechanical behavior within a standardized strain would allow better benchmarking against clinical standards.

The biological performance of the membranes was evaluated using cell proliferation (MTS) assays, cytotoxicity (LDH) release measurements, and Live/Dead viability staining. Prior to testing, membrane samples were sterilized with UV light and seeded with hGF on their smooth sides. Assessments were conducted at 1-, 3-, 7-, and 14-days post-seeding. The MTS assay results showed varied cell viability across the membranes, but the differences were not statistically significant, indicating that all tested materials are highly compatible with hGF cells. The LDH assays revealed initial significant differences in cytotoxicity which diminished by day 14, with a general decrease in LDH release in comparison to earlier observations, indicating reduced cellular stress or damage. These results were qualitatively validated by the Live/Dead staining, which showed high viability and low death rates. UV light treatment of collagen membranes has been documented not to affect their cytotoxicity negatively, but it has also been associated with altering mechanical properties, potentially affecting cell adhesion and proliferation [5,34]. Further investigation into the effects of UV light treatment is warranted. HGF were chosen and seeded on the smooth sides to mimic clinical application in which the membrane smooth side will be facing the soft tissue, rich in hGF. While this study focused on characterizing the membrane's biocompatibility and passive barrier function, the structural asymmetry of the ESM suggests potential for bioactivity, particularly on the rough outer surface. Previous studies have proposed that this side may promote biomineralization due to its fibrous collagen matrix [4]. Future work should explore the osteogenic differentiation potential and mineralization behavior of this surface, especially in comparison to conventional membranes, to assess whether ESM could actively contribute to bone regeneration in addition to serving as a barrier.

Although direct assessment of degradation was beyond the scope of this study, the degradability of ESM warrants discussion and has been reported in previous literature [10,16,20,35]. ESM is primarily composed of collagen and glycoproteins, which are known to undergo enzymatic degradation under physiological conditions. When exposed to proteolytic enzymes or fluid environments mimicking the human body, ESM gradually degrades over time. This inherent biodegradability is advantageous in regenerative applications, as it may allow the membrane to resorb naturally without requiring surgical removal. This intrinsic biodegradability is advantageous, as it may eliminate the need for membrane removal and reduce the risk of long-term foreign body response. Future investigations are warranted to characterize the in vitro and in vivo degradation kinetics of ESM more precisely, and to correlate these findings with tissue healing outcomes.

To the best of our knowledge, this study presents the first characterization of the duck ESM. Previous studies have thoroughly examined the chicken ESM, as well as the porcine-derived CM (Bio-Gide) and d-PTFE (Cytoplast). Our results are generally in line with those found in previous research in terms of thickness measurements [13,36,37], biochemical properties [12,13,33,37,38], morphological structure [12,13,31,33,37,39], wettability [13,31,37,38], and thermal properties [12,40,41], further confirming their validity. Additionally, similar to past observations [12,13,31,39], our study confirms the high biocompatibility of these membranes. The literature presents a wide variety of values for the mechanical properties of the chicken ESM and porcine-derived CM, with some reporting values higher than ours and some reporting lower values [12,13,31,33,36–38,42,43], which could be attributed to differences in experimental protocols, such as samples' preparation and strain.

Finally, this study contributes to the growing interest in sustainable, xeno-free, and culturally inclusive alternatives to mammalian-derived materials in regenerative medicine. ESM, as an avian-derived, collagen-rich by-product of the food industry, is particularly promising in this context. It is inexpensive, widely available, and generally considered safe, making it especially attractive for use in low-resource settings or among populations with ethical, cultural, or safety concerns related to mammalian sources. As a waste-derived material, ESM also aligns with global sustainability goals and circular bioeconomy principles by repurposing food industry by-products [16,44]. In line with these practical advantages, ESM has demonstrated processability into various biomedical formats – including membranes [18,19], scaffolds [45], soluble protein extracts [46], powdered forms [47], hydrogels [48], and composites [49]—broadening its translational potential. However, the pathway to clinical application requires further investigation. Key next steps include in vivo validation in appropriate models, assessment of regenerative and osteogenic potential, standardization of processing and sterilization methods, and long-term safety evaluations. Although the risk of zoonotic transmission is considered low, avian-derived biomaterials must still comply with rigorous safety and quality standards. Their regulatory classification – under frameworks such as the European Medical Device Regulation (MDR) [50] and US Food and Drug Administration (FDA) guidelines [51]—will depend on processing approaches and intended clinical use. Addressing these considerations systematically may position ESM as a viable class of resorbable barrier membranes for dental regenerative applications.

5. Conclusion

This study suggests that chicken and duck ESMs could serve as viable alternatives to commonly used membranes in GBR/GTR. ESMs are thinner than porcine-derived Bio-Gide and d-PTFE-based Cytoplast, allowing for potential enhancement of mechanical properties through techniques such as stacking. They have high collagen content and a bilayered structure that supports tissue integration and prevents epithelial cell infiltration. ESMs exhibit thermal stability, hydrophilicity, superior tensile strength (especially in duck ESM), and high compatibility with human gingival fibroblasts. This study focused on the membrane's established function as a passive barrier in GBR. Future work may investigate whether ESMs contribute additional biological cues to bone regeneration, but their mechanical and morphological characteristics alone support their use in this primary role.

Author contributions

Faisal F. Alotaibi contributed to conception, design, data acquisition, analysis, and interpretation, drafted and critically revised the manuscript; Zainab M. AlFaltawi contributed to design, data acquisition, and analysis, drafted and critically revised the manuscript; Sharon R. Oyhanart contributed to design, data acquisition, and analysis, drafted, and critically revised the manuscript; Jonathan C. Knowles contributed to design, data analysis, and interpretation, drafted, and critically revised the manuscript; Francesco D'Aiuto, contributed to conception and design, data analysis, and interpretation, drafted, and critically revised the manuscript; David Y. S. Chau contributed to conception and design, data analysis, and interpretation, drafted, and critically revised the manuscript. All authors gave final approval and agreed to be accountable for all aspects of the work.

Disclosure statement

David Chau is the CEO/CSO/Founder of ReOvum *Ltd*. Sharon Oyhanart is a clinical research advisor for ReOvum *Ltd*. ReOvum *Ltd*. made no financial contributions to this study. "The authors have no other relevant affiliations or financial involvement with any organization or entity with a financial interest in or financial conflict with the subject matter or materials discussed in the manuscript apart from those disclosed.

No writing assistance was utilized in the production of this manuscript.

Reviewer disclosures

Peer reviewers on this manuscript have no relevant financial or other relationships to disclose

Ethical declaration

Ethics approval was not required for this project. Nonetheless, all research steps were conducted in line with the principles of research ethics.

ORCID

Sharon R. Oyhanart http://orcid.org/0000-0002-4519-5652
Jonathan C. Knowles http://orcid.org/0000-0003-3917-3446
David Y. S. Chau http://orcid.org/0000-0001-9200-6749

References

Papers of special note have been highlighted as either of interest (•) or of considerable interest (••) to readers.

1. Bornstein MM, Halbritter S, Harnisch H, et al. A retrospective analysis of patients referred for implant placement to a specialty clinic: indications, surgical procedures, and early failures. Int J Oral & Maxillofacial Implants. 2008;23(6):1109–1116.
2. Dahlin C, Linde A, Gottlow J, et al. Healing of bone defects by guided tissue regeneration. Plast Reconstr Surg. 1988;81(5):672–676. doi: 10.1097/00006534-198805000-00004
   • Foundational study that introduced the principle of using barrier membranes for guided bone regeneration (GBR). It established the core concept behind the use of membranes in periodontal and implant therapy.
3. Elgali I, Omar O, Dahlin C, et al. Guided bone regeneration: materials and biological mechanisms revisited. Eur J Oral Sci. 2017;125(5):315–337. doi: 10.1111/eos.12364
   •• A comprehensive review detailing advances in GBR materials and mechanisms, offering important context for evaluating emerging biomaterials like ESM.
4. Omar O, Elgali I, Dahlin C, et al. Barrier membranes: more than the barrier effect? J Clin Periodontol. 2019;46(Suppl Suppl 21):103–123. doi: 10.1111/jcpe.13068
   • Highlights the evolving understanding of barrier membranes, including their biological activity.
5. Ren Y, Fan L, Alkildani S, et al. Barrier membranes for guided bone regeneration (GBR): a focus on recent advances in collagen membranes. Int J Mol Sci. 2022;23(23):14987. doi: 10.3390/ijms232314987
   • This review outlines current trends in collagen membrane development and limitations, supporting the rationale for exploring alternatives like ESM.
6. Alotaibi FF, Rocchietta I, Buti J, et al. Comparative evidence of different surgical techniques for the management of vertical alveolar ridge defects in terms of complications and efficacy: a systematic review and network meta-analysis. J Clin Periodontol. 2023;50(11):1487–1519. doi: 10.1111/jcpe.13850
7. Mizraji G, Davidzohn A, Gursoy M, et al. Membrane barriers for guided bone regeneration: an overview of available biomaterials. Periodontology 2000. 2023;93(1):56–76. doi: 10.1111/prd.12502
8. Alotaibi FF, Buti J, Rocchietta I, et al. Premature bone resorption in vertical ridge augmentation: a systematic review and network meta-analysis of randomised clinical trials. Clin Oral Implants Res. 2025;36(7):787–801. doi: 10.1111/clr.14435
9. Nys Y, Gautron J, Garcia-Ruiz JM, et al. Avian eggshell mineralization: biochemical and functional characterization of matrix proteins. Comptes Rendus Palevol. 2004;3(6–7):549–562.
10. Mensah RA, Salim K, Peszko K, et al. The chicken eggshell membrane: a versatile, sustainable, biological material for translational biomedical applications. Biomed Mater. 2023;18(4). doi: 10.1088/1748-605X/acd316
    •• Provides foundational insights into the properties and biomedical potential of ESM, validating its relevance as a candidate GBR membrane.
11. Sah MK, Rath SN. Soluble eggshell membrane: a natural protein to improve the properties of biomaterials used for tissue engineering applications. Mater Sci Eng: C. 2016;67:807–821. doi: 10.1016/j.msec.2016.05.005
12. Briggs E, Mensah RA, Patel KD, et al. Therapeutic application of an Ag-nanoparticle-PNIPAAm-modified eggshell membrane construct for dermal regeneration and reconstruction. Pharmaceutics. 2022;14(10):2162. doi: 10.3390/pharmaceutics14102162

13. Mensah RA, Jo SB, Kim H, et al. The eggshell membrane: a potential biomaterial for corneal wound healing. J Biomater Appl. 2021;36 (5):912–929. doi: 10.1177/08853282211024040

14. Sun P, Yan S, Zhang L, et al. Egg shell membrane as an alternative vascular patch for arterial angioplasty. Front Bioeng Biotechnol. 2022;10:843590. doi: 10.3389/fbioe.2022.843590

15. Farjah GH, Mohammdzadeh S, Javanmard MZ. The effect of lycopene in egg shell membrane guidance channel on sciatic nerve regeneration in rats. Iran J Basic Med Sci. 2020;23(4):527. doi: 10. 22038/ijbms.2020.40228.9525

16. Torres-Mansilla A, Hincke M, Voltes A, et al. Eggshell membrane as a biomaterial for bone regeneration. Polymers. 2023;15(6):1342. doi: 10.3390/polym15061342

• **Supports the emerging role of ESM in bone tissue engineering, reinforcing the novelty of this study's direct membrane evaluation approach.**

17. Adali T, Kalkan R, Karimizarandi L. The chondrocyte cell proliferation of a chitosan/silk fibroin/egg shell membrane hydrogels. Int J Biol Macromol. 2019;124:541–547. doi: 10.1016/j.ijbiomac.2018.11.226

18. Kalluri L, Duan Y. Parameter screening and optimization for a polycaprolactone-based GTR/GBR membrane using Taguchi design. Int J Mol Sci. 2022;23(15):8149. doi: 10.3390/ijms23158149

19. Kalluri L, Griggs JA, Janorkar AV, et al. Preparation and optimization of an eggshell membrane-based biomaterial for GTR applications. Dent Mater. 2024;40(4):728–738. doi: 10.1016/j.dental.2024.02.008

• **A key study on engineered ESM-based membranes, offering critical background for comparison with the native ESM materials.**

20. Dupoirieux L, Pourquier D, Picot M, et al. Comparative study of three different membranes for guided bone regeneration of rat cranial defects. Int J Oral Maxillofac Surg. 2001;30(1):58–62. doi: 10. 1054/ijom.2000.0011

21. Durmuş E, Celik I, Ozturk A, et al. Evaluation of the potential beneficial effects of ostrich eggshell combined with eggshell membranes in healing of cranial defects in rabbits. J Int Med Res. 2003;31(3):223–230. doi: 10.1177/147323000303100309

22. Bubalo M, Lazić Z, Matić S, et al. The impact of thickness of resorbable membrane of human origin on the ossification of bone defects: a pathohistologic study. Vojnosanitetski pregled. 2012;69(12):1076–1083.

23. Riaz T, Zeeshan R, Zarif F, et al. FTIR analysis of natural and synthetic collagen. Appl Spectrosc Rev. 2018;53(9):703–746.

24. Torres FG, Troncoso OP, Piaggio F, et al. Structure–property relationships of a biopolymer network: the eggshell membrane. Acta Biomater. 2010;6(9):3687–3693. doi: 10.1016/j.actbio.2010.03.014

• **Presents detailed biophysical analysis of ESM, supporting the present study's structural and mechanical characterization.**

25. Zurita-Méndez N, carbajal-De la Torre G, Flores-Merino M, et al. Development of bioactive glass- collagen- hyaluronic acid- polycaprolactone scaffolds for tissue engineering applications. Front Bioeng Biotechnol. 2022;10:825903. doi: 10.3389/fbioe.2022.825903

26. Schwarz F, Rothamel D, Herten M, et al. Angiogenesis pattern of native and cross-linked collagen membranes: an immunohistochemical study in the rat. Clin Oral Implants Res. 2006;17 (4):403–409. doi: 10.1111/j.1600-0501.2005.01225.x

27. Willershausen I, Barbeck M, Boehm N, et al. Non-cross-linked collagen type I/III materials enhance cell proliferation: in vitro and in vivo evidence. J Appl Oral Sci. 2014;22(1):29–37. doi: 10.1590/ 1678-775720130316

28. Park J-Y, Lee J-H, Cha J-K, et al. Degradation properties of a bi-layered cross-linked collagen membrane for localized bone regeneration: in vitro and in vivo study. J Korean Dent Sci. 2021;14(1):12–25. doi: 10.5856/JKDS.2021.14.1.12

29. Gutta R, Baker RA, Bartolucci AA, et al. Barrier membranes used for ridge augmentation: is there an optimal pore size? J Oral And Maxillofacial Surg. 2009;67(6):1218–1225. doi: 10.1016/j.joms.2008. 11.022

30. Wenzel RN. Resistance of solid surfaces to wetting by water industrial & engineering chemistry. 1936;28(8):988–994. doi: 10.1021/ ie50320a024

31. Shi X, Li X, Tian Y, et al. Physical, mechanical, and biological properties of collagen membranes for guided bone regeneration: a comparative in vitro study. BMC Oral Health. 2023;23(1):510. doi: 10.1186/s12903-023-03223-4

32. Schieber R, Lasserre F, Hans M, et al. Direct laser interference patterning of CoCr alloy surfaces to control endothelial cell and platelet response for cardiovascular applications. Adv Healthc Mater. 2017;6(19):1700327. doi: 10.1002/adhm.201700327

33. Ha Y-Y, Park Y-W, Kweon H, et al. Comparison of the physical properties and in vivo bioactivities of silkworm-cocoon-derived silk membrane, collagen membrane, and polytetrafluoroethylene membrane for guided bone regeneration. Macromol Res. 2014;22:1018–1023.

34. Ahmed TA, Suso H-P, Maqbool A, et al. Processed eggshell membrane powder: bioinspiration for an innovative wound healing product. Mater Sci Eng: C. 2019;95:192–203. doi: 10.1016/j.msec. 2018.10.054

35. Tsai W, Yang J, Lai C, et al. Characterization and adsorption properties of eggshells and eggshell membrane. Bioresour Technol. 2006;97(3):488–493. doi: 10.1016/j.biortech.2005.02.050

36. Ortolani E, Quadrini F, Bellisario D, et al. Mechanical qualification of collagen membranes used in dentistry. Annali dell'Istituto superiore di sanita. 2015;51(3):229–235. doi: 10.4415/ANN_15_03_11

37. Qasim SSB, Al-Asfour AA, Abuzayeda M, et al. Differences in mechanical and physicochemical properties of several PTFE membranes used in guided bone regeneration. Materials. 2023;16 (3):904. doi: 10.3390/ma16030904

38. Tunthasen R, Pripatnanont P, Meesane J. In vitro biocompatibility of a novel semi-rigid shell barrier system: as a new application for guided bone regeneration. Polymers. 2022;14(12):2451. doi: 10. 3390/polym14122451

39. Mensah RA, Trotta F, Briggs E, et al. A sustainable, green-processed, Ag-nanoparticle-incorporated eggshell-derived biomaterial for wound-healing applications. J Funct Biomater. 2023;14(9):450. doi: 10.3390/jfb14090450

40. Lai S-Q, Yue L, Li T-S, et al. The friction and wear properties of polytetrafluoroethylene filled with ultrafine diamond. Wear. 2006;260(4):462–468. doi: 10.1016/j.wear.2005.03.010

41. Hassanbhai AM, Lau CS, Wen F, et al. In vivo immune responses of cross-linked electrospun tilapia collagen membrane. Tissue Eng Part A. 2017;23(19–20):1110–1119. doi: 10.1089/ten.tea.2016.0504

42. Raz P, Brosh T, Ronen G, et al. Tensile properties of three selected collagen membranes. Biomed Res Int. 2019;2019:5163603. doi: 10. 1155/2019/5163603

43. Torres-Mansilla A, Álvarez-Lloret P, Voltes-Martínez A, et al. Apatite-coated outer layer eggshell membrane: a novel osteoinductive biohybrid composite for guided bone/tissue regeneration. Biomater Adv. 2023;154:213605. doi: 10.1016/j. bioadv.2023.213605

44. Liang X, Guo S, Kuang X, et al. Recent advancements and perspectives on processable natural biopolymers: cellulose, chitosan, eggshell membrane, and silk fibroin. Sci Bull. 2024;69(21):3444–3466. doi: 10.1016/j.scib.2024.08.023

45. Koohi-Hosseinabadi O, Shahriarirad R, Dehghanian A, et al. In-vitro and in-vivo assessment of biocompatibility and efficacy of ostrich eggshell membrane combined with platelet-rich plasma in Achilles tendon regeneration. Sci Rep. 2025;15(1):841. doi: 10.1038/s41598-025-85131-x

46. Ma Q, Piaia L, Loca D, et al. Soluble proteins from conventional and organic eggshell membranes with different proteomic profiles show similar in vitro biofunctions. J Biomed Mater Res Part A. 2025;113(1):e37848. doi: 10.1002/jbm.a.37848

47. Esmaeili S, Rahmati M, Zamani S, et al. A comparison of several separation processes for eggshell membrane powder as a natural biomaterial for skin regeneration. Skin Res And Technol. 2024;30(9): e70038. doi: 10.1111/srt.70038

48. Cengiz ZO, Durmus E, Celik I, et al. Osteoproductivity of injectable bone grafts with and without ostrich eggshell membrane protein in rabbit femur. J Funct Biomater. 2024;15(7):201. doi: 10.3390/ jfb15070201

49. Nazari N, Imani R, Nasiraie LR. Fiber/hydrogel hybrid wound dressing based on eggshell membrane containing postbiotic ingredients. Biomater Adv. 2024;165:214004. doi: 10.1016/j.bioadv.2024.214004

50. Regulation (EU) 2017/745 of the European Parliament and of the Council of 5 April 2017 on medical devices, amending Directive 2001/83/EC, Regulation (EC) No 178/2002 and Regulation (EC) No 1223/2009 and repealing Council Directives 90/385/EEC and 93/42/EEC (OJ L 117 5.5.2017, p. 1). Official Journal of the European Union; 2017.

51. Van Norman GA. Drugs, devices, and the FDA: part 2: an overview of approval processes: fDA approval of medical devices. JACC: Basic To Transl Sci. 2016;1(4):277–287. doi: 10.1016/j.jacbts.2016.03.009